Thermo-Acoustic Instability in the Horizontal Rijke Tube

Woo-Seog Song, Seungbae Lee*
Department of Mechanical Engineering, College of Engineering, Inha University, Incheon 402-751, Korea
Dong-Shin Shin
Department of Mechanical System Desighn Engineering, College of Engineering, Hongik University, Seoul 121-791, Korea
Yang Na
CAESIT, Department of Mechanical Engineering, Konkuk University, Seoul 143-701, Korea

The instability curve of a Rijke tube system was obtained accurately by following different paths of heat power and flow-rate for three regions and by defining its locus from the criterion based on the measured sound pressure levels. The unstable limits in the region of flow-rate lower than that at the minimal power are compared with previous data. To observe the effect of turbulence on the unstable limits, inflow turbulence was introduced by placing a bundle of circular cylinders upstream of the heating part ($50<Re_d<700$). The large-amplitude inflow fluctuation may delay the transition of the chamber acoustic mode to the unstable zone even at a sufficient power.

Key Words : Thermo-acoustic Instability, Rijke Tube, Inflow Turbulence

Nomenclature

p' : Pressure perturbation
$\dot{Q}'$: Fluctuation of heat release rate
p_0 : Mean ambient pressure
V : Chamber volume
T : Cycle period
ΔE : Energy supplied to acoustic mode
$S_{A\min}$: Minimal SPL in stable, low flow-rate region
$S_{A\max}$: Maximum SPL in unstable, low flow-rate region
$S_{B\min}$: Minimal SPL in stable, high flow-rate region
$S_{B\max}$: Maximum SPL in unstable, high flow-rate region

* Corresponding Author,
E-mail : sbaelee@inha.ac.kr
TEL : +82-32-860-7325; **FAX** : +82-32-868-1716
School of Mechanical Engineering, Inha University, 253, Yonghyun-dong, Nam-gu, Incheon 402-751, Korea. (Manuscript **Received** March 2, 2006; **Revised** March 30, 2006)

M_{AI} : Transition zone of instability limits in low flow-rate
M_{BI} : Transition zone of instability limits in high flow-rate
m_{AL} : Minimum mass flow-rate in M_{AI}
m_{AH} : Maximum mass flow-rate in M_{AI}
m_{BL} : Minimum mass flow-rate in M_{BI}
m_{BH} : Maximum mass flow-rate in M_{BI}
d : Diameter of cylinder
Re_d : Reynold number based on cylinder diameter
u_i : Instantaneous flow velocity
U_0 : Time-mean flow speed
u_i' : Fluctuating velocity
N : Total data number
Tu : Turbulence intensity (%)

Greeks

λ : Wavelength of eigen mode in tube
γ : Gas constant
σ : Root mean square of fluctuating velocity

1. Introduction

The importance of thermo-acoustic instability has been widely recognized in practical combustion problems. The typical examples where this type of instability is involved are propulsion systems, lean-burn combustors for low-emission, commercial combustors of high noise-emission issue, and thermo-acoustic engines. Especially, the propulsion rocket and the gas-turbine engine are especially vulnerable to combustion instability. In this case, the pressure and the flow fluctuations in the motor induce unwanted vibration and increase heat transfer accompanied by a rapid drop of propulsion efficiency, leading to malfunction or serious damage to the system.

Thermo-acoustic oscillation was observed first by Higgins (1802). He found the singing of the flame when it was located inside the tube an open end and a closed end Rijke (1859) experimented with a both open-ended vertical tube. When the mesh for heating connected to the electricity was located in the upper part of the vertical tube, no thermo-acoustic oscillation was observed, but when it was in the lower part, severe vibration occurred. Rayleigh (1878) suggested the famous criterion that explained the experimental results of Higgins and Rijke qualitatively. Lehmann (1937) examined a qualitative model that used a flat coil heater to explain the Rijke tube phenomenon.

Kerwin (1954) studied the acoustic growth-rate α in terms of heat source location x by using a ribbon heater in the Rijke tube. Maling (1963) measured the lowest average speed for the onset of instability by using a nichrome ribbon heater in the Rijke tube and compared this speed with that obtained by Carrier's heated ribbon model. Saito (1965) tried to predict the acoustic growth-rate α by integrating a linearized conservation equation with respect to the distance across the heater. Katto and Sajiki (1977) extended the previous researches by measuring the stability limits according to the supply power, the heat source position, and the average flow-rate. Madarame (1981) proposed an α prediction model based on the average flow-rate and the source temperature by measuring the stability limits for the tube with heated wire spirals. Kwon and Lee (1985) studied the stability limit of the Rijke tube oscillation by using a heater wire to fluctuate heat transfer and generate a thermo-acoustic power. Furthermore, Heckl (1988) tried to control the oscillation amplitude and phase change by using a speaker at the exit of the Rijke tube, and derived the energy balance and the eigen-value equations for the prediction of α. Cho and Lee (1999) applied a Filtered-X LMS algorithm to control the thermo-acoustic instability in the Rijke tube combustor adaptively.

Recently, the boundary locus for the thermo-acoustic instability has been used to search for the important parameters affecting the thermo-acoustic characteristics in the tube. In this respect, the horizontal Rijke tube is assumed to provide unstable limits more accurately for the given properties of the system. This precise experimental data can be used to confirm the mathematical modeling for thermo-acoustics characteristics. On the other hand, the thermo-acoustic instability is very sensitive to the system properties and may change depending on the experimental condition. Though the instability boundary has been by many experimentalists, e.g. Matveev (2003), with the help of high-accuracy equipment and improved data processing technique, it still needs to be studied more precisely with respect to complex mechanisms.

Therefore, the instability locus is precisely determined by defining different paths of heat release and flow-rate for three regions, and the effect of incoming turbulence on this locus is discussed in this study.

2. Experimental Apparatus and Measurements

2.1 Rijke tube apparatus

Several simple models have been suggested to describe the thermo-acoustic phenomena. To treat the thermo-acoustic instability problem theoretically or experimentally, the vertical type of Rijke tube, in which the gauze of wires heated by flames was placed in the lower part of the tube,

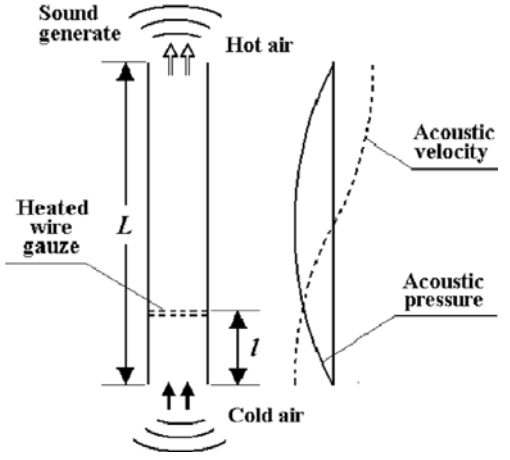

Fig. 1 Characteristics of Rijke tube

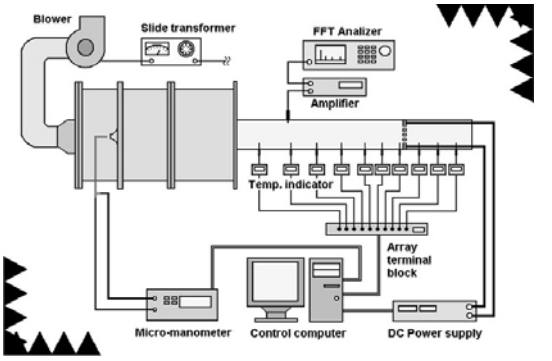

Fig. 2 Experimental setup of horizontal Rijke tube

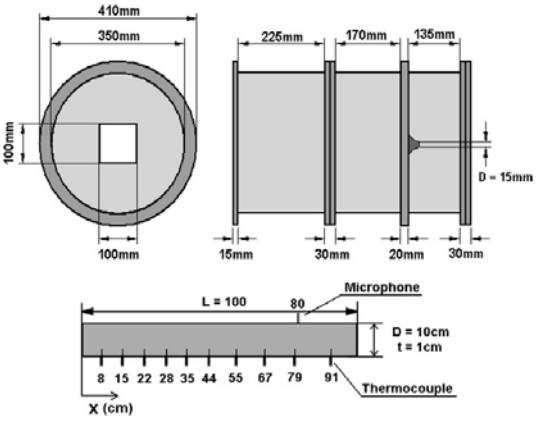

Fig. 3 Dimensions of chamber and measuring setup

was devised originally.

Figure 1 shows the acoustic characteristics in the standard Rijke Tube. Heating the gauze in the tube creates naturally convective fluid motion due to the density difference between the heating part and the ambient air in the tube. When the heating is sufficient to supply energy to the system, the vibration of air inside the tube is amplified by repeating the procedure of adding heat at the maximum compression of air and subtracting heat at the maximum expansion of air through a feedback loop.

The theoretical explanation about the acoustic oscillation in the tube was given by Culick (1976) as in Eq. (1).

$$\Delta E=\frac{\gamma-1}{p_0\gamma}\int_V dv\int_t^{t+T} p'\dot{Q}'dt \qquad (1)$$

where p', $\dot{Q}'$, γ, p_0, V, and T are the pressure perturbation, the fluctuation of the heat release rate, the gas constant, the mean ambient pressure, the chamber volume, and the cycle period, respectively. Equation (1) states that the system becomes unstable when ΔE has a positive value, and that the instability is determined by the product of fluctuating pressure and fluctuating heat release rate. In other words, the system is most unstable when the fluctuating pressure and the fluctuating heat release rate have the same phase.

2.2 Experimental set-up and measurements

All the experiments were conducted in an anechoic chamber, which has the background SPL (Sound Pressure Level) below 20dBA. The experimental set-up of the horizontal Rijke tube is shown in Fig. 2, and the dimensions of the tube and the settling chamber are given in Fig. 3. Air is drawn from the surroundings by a blower and is controlled independently from the heat supply. The experimental set-up was based on that of Matveev (2003) to compare the thermo-acoustic instability locus obtained from the experimental set-up with that of Matveev, quantitatively.

The measurement system is composed of a power supply module, a flow control module, and a measuring sensor module. First the heating part should endure without distortion for a long time at a very high temperature and extreme power uniformly supplied to the cross-section. Codierite of ceramic material was machined in a

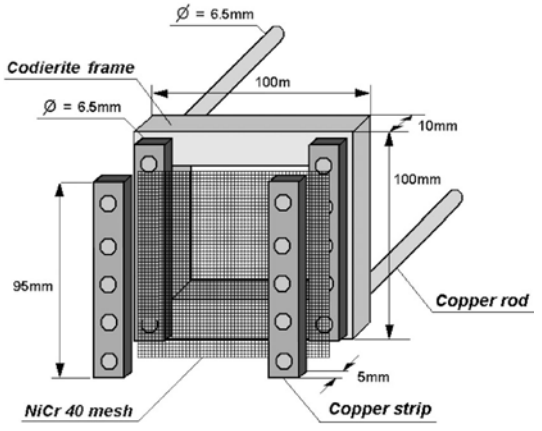

Fig. 4 Setup of heating part

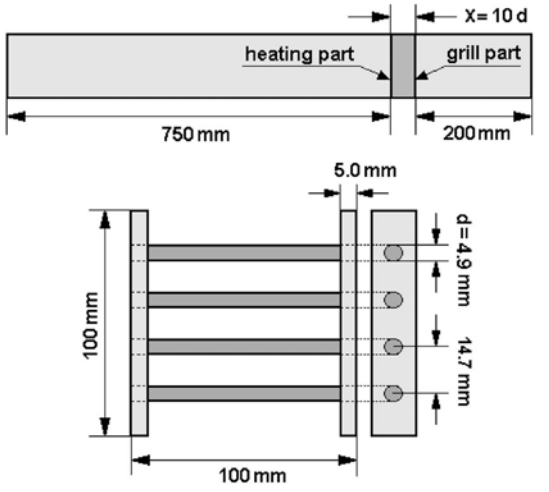

Fig. 5 Setup of grill part

square frame to support the heat-supply portion at high temperature and to connect four copper columns to provide parallel currents to a 40-mesh made of nichrome for the uniform distribution of temperature. The heating part assembly and its frame are shown in Fig. 4. The frame was fixed to the tube so that it would not vibrate from the thermo-acoustic resonance. The power was supplied by a DCS-3KW model of DC 8V and 375A at the maximum output.

To measure and control the air mass flow-rate in the tube accurately, an ISO nozzle of 15 mm diameter was designed and installed inside the settling chamber. The air velocity generated by a sirocco fan was measured by using a pitot tube and a micro-manometer (FC0510 model). The air mass flow-rate was accurately measured by the nozzle for the range of concern. Figure 5 shows set-up and geometry of the cylinder grill set-up designed for generating inflow fluctuations to the heating mesh.

To measure the acoustic characteristics in the tube, an acoustic pressure sensor (PCB model 112A04) suitable for high-pressure and high-temperature environment, a charge amplifier (PCB model 422E11), and a signal conditioner (PCB model 480E09) were used. The sensor was placed 800 mm downstream of the heating mesh and its signal was A/D converted by a DAQ board (NI PCI model 6071E).

Ten k-type thermo-couples were placed at 80, 150, 220, 280, 350, 440, 550, 670, 790, 910 mm downstream of the heating mesh to measure the air temperatures in the tube, as shown in Fig. 2. The flow-rate, the electric power, and temperatures were stored simultaneously with the acoustic signals in a 32-bit personal computer by the DAQ board and a terminal block (NI model BNC 2090). The measurment system was effective and accurate for simple modeling.

3. Experimental Results and Discussion

3.1 Definition of unstable limits

In the unstable region of the Rijke Tube, pressure level at the mode determined by the boundary condition significantly increased. For example, the first mode in 1 meter-long and both open-ended tube occurred as a standing wave of $\lambda/2$ in the tube near 170 Hz. Figure 6 shows the rapidly growing pressure amplitude as resonance formed inside the tube. The maximum pressure amplitude depended on the heating power and the flow-rate in the tube. As an example case, the mass flow-rates were varied 11 times in the range of 0.77～4.28 g/s at a fixed heating power of 730W, as shown in Fig. 7. The acoustic pressure increases abruptly by 60dB when the chamber acoustic mode from the stable, low and high flow-rate regions to the unstable, mid flow-rate region. Based on this observation, limiting cases where

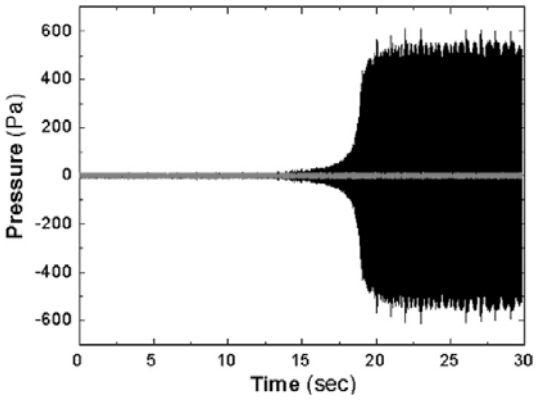

Fig. 6 Sound pressure signal showing typical development of thermo-acoustic instability

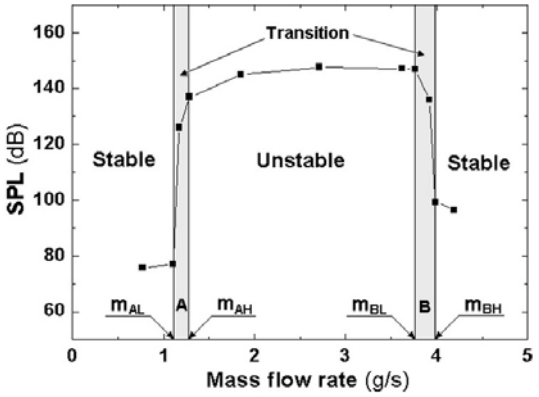

Fig. 7 Sound pressure level vs. mass flow-rate (power is fixed at 730W and mass flow-rate is varied from 0.77 g/s to 4.28 g/s)

the air column starts to become unstable may exist, and the limiting case in the transition zone may also be very sensitive to the system parameters. Therefore, unstable limit should be clearly defined for the further discussion. In this study, the unstable region was determined by measuring the maximum and minimum levels of acoustic pressures in the transition zone. The measured maximum and minimum SPL's in stable and unstable regions are defined as $S_{A\min}$, $S_{B\min}$ and $S_{A\max}$, $S_{B\max}$, respectively. M_{AI} and M_{BI} represent unstable transition regions defined by using m_{AL}, m_{AH}, and m_{BL}, m_{BH} denoted in Fig. 7, all of which are functions of combined sound pressure levels, as shown in Table 1.

Table 1 Definition of unstable limit

	$m_{AL} \le M_{AI} \le m_{AH}$
m_{AL}	$f\{S_{A\min}+(S_{A\min}-S_{A\max})\times 0.30\}$
m_{AH}	$f\{S_{A\min}+(S_{A\min}-S_{A\max})\times 0.70\}$
	$m_{BL} \le M_{BI} \le m_{BH}$
m_{BL}	$f\{S_{B\min}+(S_{B\min}-S_{B\max})\times 0.30\}$
m_{BH}	$f\{S_{B\min}+(S_{B\min}-S_{B\max})\times 0.70\}$

(f means a function of { })

3.2 Effect of temperature on instability limit curve

In this experiment, the heating mesh was located at the position of $L/4$ (L: tube length) from the entrance of the tube. The heat transfer between inlet of aluminum duct and the air was minimized by cooling the aluminum duct to maintain the incoming air-temperature between 27℃ and 30℃. Otherwise the change of air temperature may affect the instability curve, significantly. When we supply electric power to the system up to the desired level, the increase rate of power near the unstable region must be minimized to keep the system in a quasi-steady state. Thus, the fast increase of heating before reaching the stable region and the slow increase of heating in the transition zone help the unstable limit to be determined within the specified accuracy. But the tube should not be heated for a long time because prolonged heating may induce excessive heat transfer and shift the system to a different mode. The temperature increase of the air passing the flow-measuring nozzle may increase the mass flow-rate of air up to 14% even at the same air speed due to the air density drop in the region of high-power and high-flow.

3.3 Effect of supply paths on instability limit curve

Since the reporting of the unstable limit curves of the horizontal Rijke tube most their measurements were found incomsistent in the low flow-rate region due to the broad error-bound and the inevitable restriction of rapid mode-change when high power is applied to the air of low mass flow-rate. This kind of defect may lead to incorrect modeling of thermo-acoustic characteristics. In

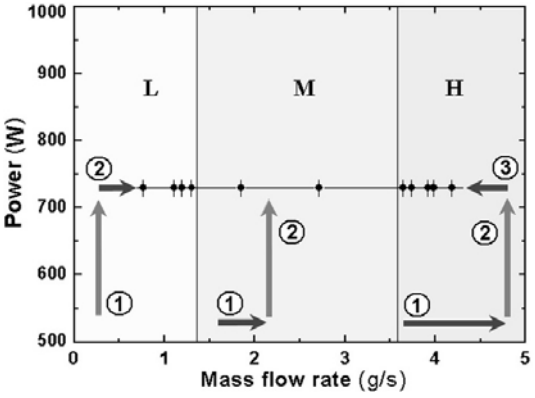

Fig. 8 Searching path on the domain of power and flow-rate

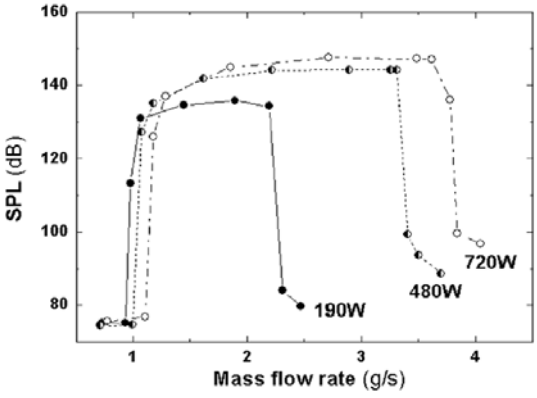

Fig. 9 Measured acoustic pressure level by changing the flow-rate at each constant power

this study, to overcome the this difficulty, three different paths for low, mid, and high flow-rate regions are defined, as indicated in the example of 730W power supply shown in Fig. 8. In the case of low flow-rate below the minimum power limit point, the expected power limit is approached by following line ① and then line ② of increasing the flow-rate in the L-region, as in Fig. 8. The limit point is determined by the definition given in Table 1, based on 200 times averaging of sound pressure levels. In the case of high flow-rate, the sufficiently stable point is firstly selected.; then the flow-rate is increased along the line ①; the power is supplied along line ② up to expected power limit; and the flow-rate is decreased slowly on line ③ until the limit point is detected. At the medium flow-rate, the expected flow-rate follows along line ① and then the power is increased along line ② with checking the acoustic pressure levels in the unstable states. In this range, the unstable mode occurs independent of the path, nevertheless, the above method is selected for the systematic approach.

Figure 9 shows the measured acoustic pressures inside the tube for three heat-supply cases of 190W, 480W, and 720W, all of which are searched along the selected paths. In Fig. 10, the instability locus is summarized for the measurable range of the supply power. As can be seen, the instability limit curve is a double-valued function of the mass flow-rate in the low flow-rate region. To compare the curve with that of Matveev (2003),

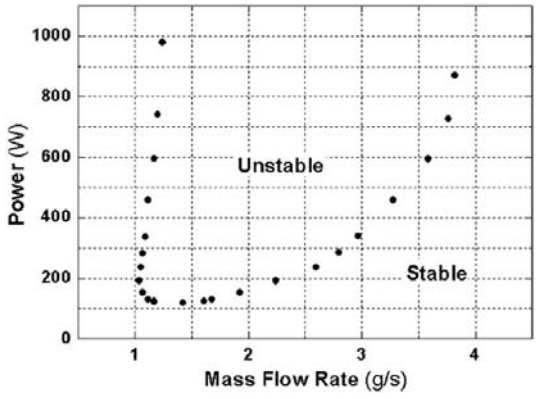

Fig. 10 Measured instability limit curve

the flow-rate and the power are given in the form of flux by dividing them by each effective heating area in Fig. 11. Two experiments coincide with each other in the region between the minimal power point ($0.018\ g/s\,cm^2$, $2.438\ W/cm^2$) and the highest flow-rate point ($0.068\ g/s\,cm^2$, $17.765\ W/cm^2$). But in the low flow-rate region where the mass flux is less than $0.018\ g/s\,cm^2$, the measured locus can hardly be compared with the previous data due to the limitation of their searching methods. The instability curve with a steep positive slope are clearly seen in the low flow-rate region, and the parabolic locus were obtained in the previous researches. When the system is heated by 439W at the mass flow-rate of 0.1 g/s and then the power is decreased to 338W and 249W step by step at a fixed mass flow-rate, the instability characteristics of the steep and positive

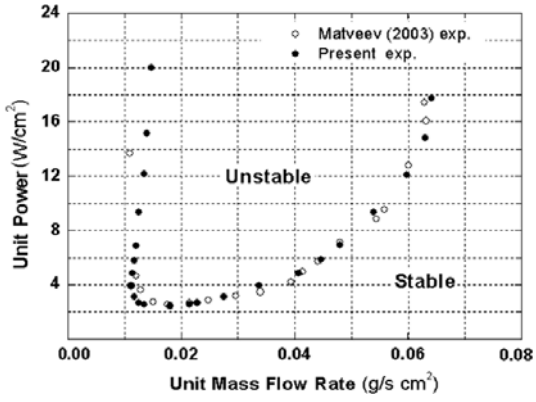

Fig. 11 Comparison of normalized instability limit curve with that of Matveev(2003)

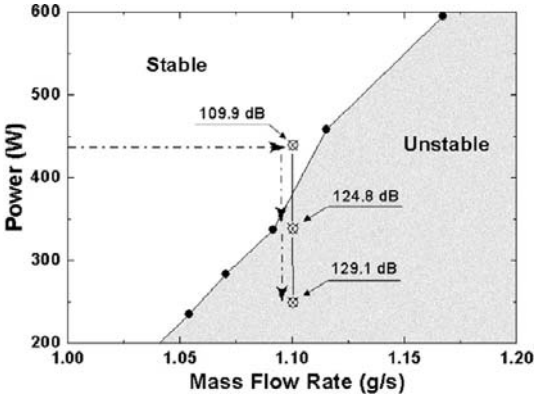

Fig. 12 Limit curve approach with flow-rate fixed in the low flow-rate region

slope are observed, as shown in Fig. 12.

3.4 Effect of inflow turbulence on limit curve

In this part of experiment, the effect of randomly fluctuating inflow on the thermo-acoustic instability is studied by controlling the incoming turbulence intensity into the heating mesh, as shown in Fig. 5. The turbulence intensity was measured by using a hot-wire anemometry and the measurement accuracy was confirmed by comparing the velocity obtained by the pitot tube just downstream of the nozzle with the incoming velocity obtained by the hot-wire sensor near the heating mesh center. The linearity between the velocities was observed except in the low flow-rate region of the grill-installed case, as shown in

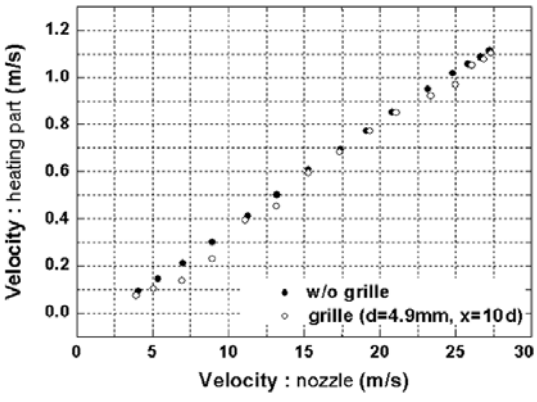

Fig. 13 Velocity measurements near nozzle and heating mesh

Fig. 13. The Reynolds number Re_d of the cylinder which is based on the mean incoming speed and the cylinder diameter, for the grill ranged from 50 to 700, which according to Fey (1998), indicates that the flow may change from larminar parallel-shedding mode to B mode shedding.

The turbulence intensity was computed by using Eqs. (2).

$$\sigma=\sqrt{\frac{1}{N}\sum_{i=1}^{N}u_i'^2},\ (u_i'=U_0-u_i)$$
$$Tu=\frac{\sigma}{U_o}\times 100\% \tag{2}$$

where u_i and U_0 are instantaneous and mean incoming velocities into the heating mesh, respectively.

Figure 14 shows the measured turbulence intensities for two cases of grill and no-grill. For the grill case, turbulence intensity increase up to 15% and reached an plateau after Re_d=280, whereas for the no grill case, the turbulence intensity level was around 4%. The limit curves behave similarly, but deviate from each other significantly at the mass flow-rate over 2.5 g/s, as shown in Fig. 15. The acoustic pressure inside the tube for the no-grill case increased significantly, while that for the grill case stayed in the stable mode with repeating fluctuation, at the same operation point of 602.8 W and 3.495 g/s, as shown in Fig. 16. It should be noted that the transition process needs a sufficient and steady power-supply for the complete coupling of acoustic mode

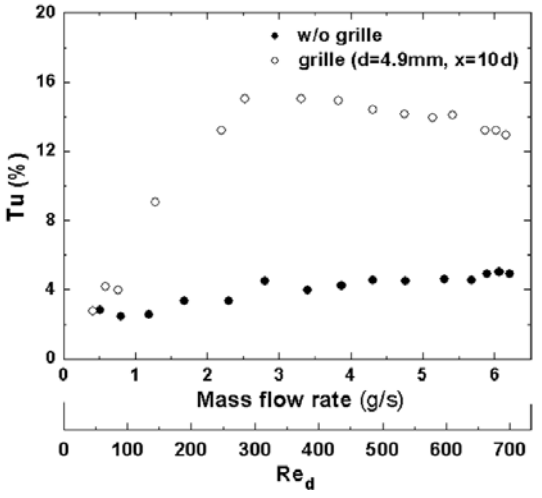

Fig. 14 Turbulence intensity comparison for grill and no-grill cases

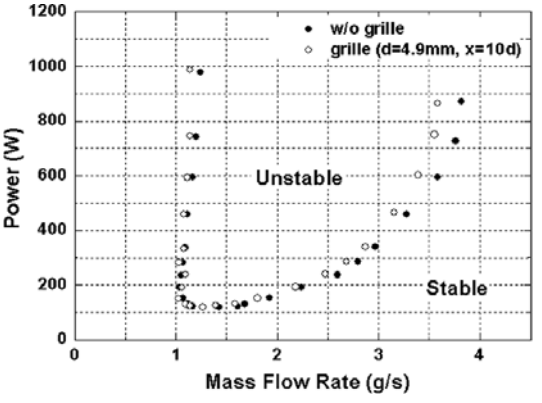

Fig. 15 Instability limit curves for grill and no-grill cases

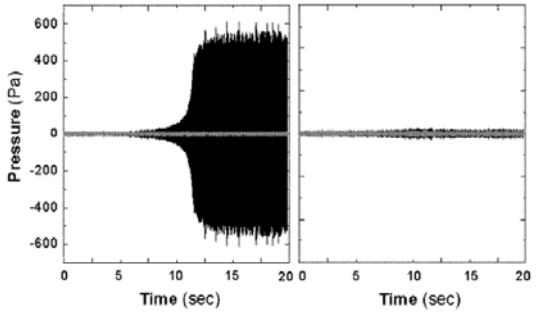

Fig. 16 Acoustic pressures in time at same power and same flow-rate for grill and no-grill cases

and heat release fluctuation. The large-amplitude inflow fluctuation by turbulence delays the strong coupling of acoustic mode and heat release even at sufficient power.

4. Conclusions

In this experiment, three different regions were defined at each heating power, and the instability point for each unstable region was approached by following the designated path. The measured instability limit curve was found to be very close to that of Matveev (2003) in the high flow-rate region, but to have quite a different slope in the low flow-rate region below the least power limit point.

The perturbed incoming flow up to 15% of turbulence intensity by the upstream grill of the cylinders stabilizes the system. The instability curve when the Re_d is greater than 280 and the incoming turbulence intensity is established around 15% starts to deviate significantly from that of no-grill case. The incoming flow perturbation of high amplitude and its very short period compared to the time needed for the normal transition stabilizes the system stable even at sufficient power-supply for acoustic resonance.

Acknowledgments

This research was supported by the Grant No. R01-2004-000-10041-0 from the Basic Research Program of the Korea Science & Engineering Foundation.

References

Cho, S., Lee, Y. and Lee, S., 1999, "Active Control of Thermoacoustic Instability in Cylindrical Ducted Combustor," 35th Aerospace Science Meeting and Exhibit, Reno, CA, Jan. 12-15.

Culick, F. E. C., 1976, "Nonlinear Behavior of Acoustic Waves in Combustion Chambers Parts I and II," *Acta Astronautica*, Vol. 3, pp. 714~757.

Fey, U., Konig, M. and Eckelmann, H., 1998, "A new Strouhal-Reynolds-Number Relationship for the Circular Cylinder in the Range

$47 \ll 2 \times 10^5$," *Physics of Fluids*, Vol. 10, No. 7, pp. 1547～1579.

Heckl, M. A., 1988, "Active Control of the Noise From a Rijke Tube," *Journal of Sound and Vibration*, Vol. 124, pp. 117～133.

Higgins, B., 1802, *Journal of Natural Philosophy and Chemical Arts* 1 : 129.

Katto, Y. and Sajiki, A., 1977, "Onset of Oscillation of a Gas-column in a Tube Due to the Existence of Heat-conduction Field," *Bulletin of the Japanese Society of Mechanical Engineers*, Vol. 20, No. 147, pp. 1161～1168.

Kerwin, E. M., 1954, *Jr. Thesis*, Massachusetts Institye of Technology, Cambridge, MA.

Kwon, Y.-P. and Lee, B.-H., 1985, "Stability of the Rijke Thermoacoustic Oscillation," *Journal of Acoustical Society of America*, Vol. 78, No. 4, pp. 1414～1420.

Lehmann, K. O., 1937, Uber die theory der netztone, *Annalen der Physik* 29, pp. 527～555.

Madarame, H., 1981, "Thermally Induced Acoustic Oscillations in a Pipe," *Bulletin of the Japanese Society of Mechanical Engineers*, Vol. 24, No. 195, pp. 1626～1633.

Maling, G. C., 1963, "Simplified Analysis of the Rijke Phenomenon," *Journal of the Acoustical Society of America*, Vol. 35, No. 7, pp. 1058～1060.

Matveev, K. I. and Culcik, F. E. C., 2003, "A Study of the Transition to Instability in a Rijke Tube With axial Temperature Gradient," *Journal of Sound and Vibration*, Vol. 264, pp. 689～706.

Rayleigh, J. W. S., 1945, *The Theory of Sound*, Dover Publications.

Rijke, P. L., 1859, *Philosophical Magazine* 17, pp. 419.

Saito, T., 1965, "Vibrations of Air-columns Excited by Heat Supply," *Bulletin of the Japanese Society of Mechanical Engineers*, Vol. 8, No. 32, pp. 651～659.